AIMS Mathematics, 9(8): 21255–21272.
DOI: 10.3934/math.20241032
Received: 15 April 2024
Revised: 25 May 2024
Accepted: 06 June 2024
Published: 01 July 2024

http://www.aimspress.com/journal/Math

Research article

A new model for COVID-19 in the post-pandemic era

Xiaoying Pan and Longkun Tang*

School of Mathematical Sciences, Huaqiao University, Quanzhou 362021, China

* **Correspondence:** Email: tomlk@hqu.edu.cn.

Abstract: Coronavirus disease 2019 (COVID-19) in the early days of the pandemic had significant differences in propagation and contact modes from those in the post-pandemic era. In order to capture the real dynamic behavior of COVID-19 propagation in the post-pandemic era, this study takes into account groups with the awareness of self-protection (including taking self-quarantine measures), as well as with loss of immunity, and establishes a new SLEIRS (Susceptible, Low-risk, Asymptomatic infected, Infected and Recovered) epidemic model with births and deaths on the basis of an SEIR model through adding compartment for low-risk groups. For the proposed model, we proved the existence of equilibrium points, identified the stability condition of equilibrium points as well as the basic regeneration number, and verified the proposed theoretical results with numerical simulations. Furthermore, the analysis of the impact of parameters on disease transmission has revealed that detecting the asymptomatic infected is a good measure to prevent and control the disease transmission. More practically, we used the particle swarm optimization (PSO) algorithm to estimate the model parameters based on the real epidemic data, and we then applied the model with estimated parameters to make predictions for the half-a-month epidemic in 2022. Results show the prediction and the estimated parameters are basically consistent with the practical situation, indicating that the proposed model has good capability in short-term prediction for COVID-19 in the post-pandemic.

Keywords: epidemic models; COVID-19; nonlinear dynamics; parameter estimation
Mathematics Subject Classification: 92B05, 93D05

1. Introduction

It is well known that coronavirus disease 2019 (COVID-19) has swept all over the world, and has resulted in immeasurable losses in social and economic development as well as in human life and health. So, it is of extremely great significance to prevent and control the epidemic spread. This stimulates numerous investigations and studies on the COVID-19 epidemic, including the immunology [1, 2], the propagation mechanism [3–6], and the epidemic prediction and

prevention [7–10] of COVID-19.

Among these, studies in the area of disease propagation mechanisms are mainly analyzed qualitatively through the development of differential equations. As a fundamental tool in the study of diverse dynamics, research on the theoretical aspects of differential equations has consistently been a subject of great interest. In the study conducted by Rezapour et al. [11], a new structure of an applied model of a thermostat is defined using generalized ψ-operators, and based on functional analysis techniques, the non-existence and existence of mild solutions for such a generalized ψ-system are established. Shah et al. [12] established some theoretical and numerical results for a nonlinear dynamical system under Caputo fractional order derivative, and the system addresses an infectious disease like COVID-19. Turab et al. [13] studied a particular type of iterative second-order differential equation and used the Banach fixed point theorem to find the existence and uniqueness of a solution to the proposed differential equation.

For model-based investigations, some classical epidemic models developed early, such as SIS [14], SIR [15], and SEIR [16], are improved to better describe and study the dynamical behavior of COVID-19 [17–19]. For example, Cooper et al. [20] proposed an SIR model with the feature of communities and provided a theoretical framework for studying the epidemic spread within the community. Piovella [21] simplified the SEIR epidemic model and gave the analytic peak value of infected COVID-19 population as well as the asymptotic value. Ivorra et al. [22] proposed a θ-SEIHRD model where θ is the rate of detected cases to the actual total infected COVID-19 cases and investigated the impact of the detected rate θ on the size of COVID-19 in China. [23] proposed an information dissemination model, the M-SDI (Multiple-Information Susceptible-Discussing-Immune) model, to describe the dissemination of public opinion caused by COVID-19 data on China's Sina Weibo. Sintunavarat et al. [24] proposed a time-fractional ($S_P E_P I_P^A I_P^{S_P} H_P R_P$) model of the COVID-19 pandemic disease in the sense of the ABC-fractional operator. Furthermore, a stability analysis in the context of Ulam-Hyers and the generalized Ulam-Hyers criterion was also discussed. Rihan et al. [25] provided an epidemic SIR model with long-range temporal memory and formulated a new set of sufficient conditions that guarantee the global stability of the steady states.

For the investigations on the basis of models combined with the real epidemic data, some researchers improved the infectious disease model and estimated and predicted the epidemic spread based on the real COVID-19 epidemic data [26]. Among them, He et al. [27] presented an SEIR model with control strategies (such as hospitals, quarantine, and external inputs) and used the measured COVID-19 data in Hubei Province of China to estimat the model parameters via the particle swarm optimization (PSO) algorithm. According to the epidemic situation in Indonesia, Annas et al. [28] improved the SEIR model by imbedding vaccination and isolation factors into model parameters. [29] proposed an SUQC model to characterize the dynamics of COVID-19 and predicted and showed the intervention effects of parametric control measures, based on the daily published data of confirmed cases in several cities in China. Raslan [30] proposed an SEQIHR model, and based on that they analyzed the effect of precautionary measures on the dynamical behaviors, as well as predicted COVID-19 in Egypt, showing the prediction result is basically consistent with actual reported data, and a long enough quarantine period can control the outbreak effectively. Rihan et al. [31] proposed a stochastic epidemic model, with time-delays, Susceptible-Infected-Asymptomatic-Quarantined-Recovered (SIAQR). Numerical simulations show that the proposed stochastic delay differential model is consistent with the physical sensitivity and fluctuation of the real observations.

However, the vast majority of models in the abovementioned works ignore the group with self-protection consciousness, the asymptomatic infected group, and those losing immunity. It is confirmed that these groups are ubiquitous in the post-pandemic era, and the natural births and deaths of the population is a non-negligible factor in the long-term epidemic. So far, the propagation mechanism of COVID-19 and its variants are still unclear especially in the post-pandemic era.

Motivated by the abovementioned information, in view of the characteristics of epidemic propagation in the post-pandemic era, this paper introduces a low-risk compartment with self-protection consciousness, considers the case of the lost-immunity individuals in the recovered, on the basis of an SEIR model, and proposes a new SLEIRS model with the birth-death rate. Compared with the SEIR model, the SLIERS model is more suitable for characterizing the state feature of COVID-19 propagation. Further, we theoretically and numerically analyze the stability of equilibrium points on the proposed model, as well as the influence of model parameters on the epidemic dynamics, showing that the enhanced detection of the asymptomatic infected can effectively prevent and control the epidemic spread. Also, the real COVID-19 data in China is used to estimate the model parameters and predict the epidemic.

The rest of this paper is organized as follows. In Section 2, a new SLEIRS model with birth-death rates is proposed. The dynamical behavior analysis of the proposed model is given in Section 3, including the existence and the stability of equilibrium points and the influence of model parameters on the basic regeneration number. In Section 4, numerical simulations are provided to validate the theoretical result, and the real epidemic data in the post-pandemic is used to estimate the model parameters via the PSO algorithm and then make predictions based on the proposed model with estimated parameters. Finally, the conclusion and discussion are given in Section 5.

2. SLEIRS model

In consideration of the transmission characteristics of COVID-19, the paper introduces a low-risk compartment (denoted "L") based on the traditional SEIR model and develops a new COVID-19 epidemic model with birth and death rates, namely the SLEIRS model, which has five compartments: Susceptible (S), low-risk (L), asymptomatic infected (E), infected (I), and recovered (R). The proposed SLEIRS model is constructed based on the following basic assumptions:

(1) The total population N always keeps constant, i.e., $S(t) + L(t) + E(t) + I(t) + R(t) = N$.

(2) The birth rate into and death rate from the susceptible and low-risk compartments are assumed to be identical for keeping the constant total population.

(3) The infected probability of susceptible individuals is assumed to be greater than that of low-risk individuals, namely, $\alpha > \beta$, due to the stronger protection awareness of low-risk individuals.

(4) Recovered individuals may be turned into susceptible and low-risk individuals with the loss of immunity probability of σ.

Under the above assumptions, the propagation process of states in the SLEIRS model is described by Figure 1, and the parameters and state variables are illustrated in Table 1.

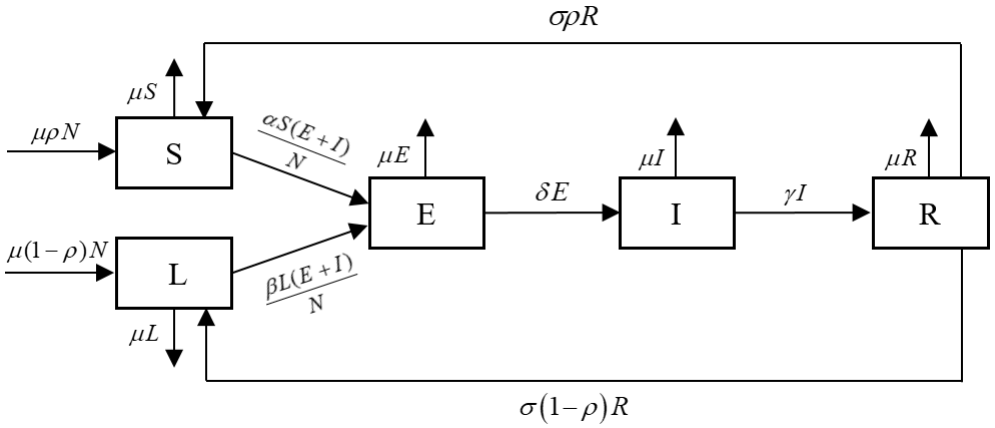

Figure 1. The propagation diagram of SLEIRS model.

Table 1. The list of model variables and parameters.

Variables/Parameters	Definitions
N	Total population
S	Susceptible population
L	Low-risk population
E	Asymptomatic infected population
I	Infected population
R	Recovered population
μ	The rate of natural births or deaths
ρ	The rate that the recovered transfer to the susceptible
α	The infected rate of the susceptible
β	The infected rate of the low-risk
δ	The rate that the asymptomatic infected break out into the infected
γ	The recovered rate of infected individuals
σ	The rate that the recovered lose immunity

According to the propagation diagram shown in Figure 1, it is easy to obtain the following dynamics equation describing the propagation behavior of the SLEIR model. The model (2.1) depicts the process of birth, natural death, infection, outbreak, recovery, and loss of immunity in each compartment. The number of people in each compartment is transferred from the remaining compartments with varying probability, and also removed with a certain probability. This results in a change in the number of people in the compartments, which is abstracted into mathematical expressions as the kinetic equations shown in model (2.1).

$$\begin{cases} \dfrac{dS}{dt} = \mu\rho N + \sigma\rho R - \dfrac{\alpha S(E+I)}{N} - \mu S, \\ \dfrac{dL}{dt} = \mu(1-\rho)N + \sigma(1-\rho)R - \dfrac{\beta L(E+I)}{N} - \mu L, \\ \dfrac{dE}{dt} = \dfrac{\alpha S(E+I)}{N} + \dfrac{\beta L(E+I)}{N} - \delta E - \mu E, \\ \dfrac{dI}{dt} = \delta E - \gamma I - \mu I, \\ \dfrac{dR}{dt} = \gamma I - \sigma R - \mu R. \end{cases} \tag{2.1}$$

Divided by the total population at each equality of model (2.1), it is rewritten as

$$\begin{cases} \dfrac{dS}{dt} = \mu\rho + \sigma\rho R - \alpha S(E+I) - \mu S, \\ \dfrac{dL}{dt} = \mu(1-\rho) + \sigma(1-\rho)R - \beta L(E+I) - \mu L, \\ \dfrac{dE}{dt} = \alpha S(E+I) + \beta L(E+I) - \delta E - \mu E, \\ \dfrac{dI}{dt} = \delta E - \gamma I - \mu I, \\ \dfrac{dR}{dt} = \gamma I - \sigma R - \mu R, \end{cases} \tag{2.2}$$

where $0 \le S, L, E, I, R \le 1$, $S + L + E + I + R = 1$, and it is not difficult to prove the positive invariant set $\Omega = \{(S, L, E, I, R) \in \mathrm{R}_+^5 | 0 \le S, L, E, I, R \le 1, S + L + E + I + R = 1\}$.

3. Dynamics analysis of SLEIRS model

3.1. Equilibrium and the basic reproduction number

Let the right-hand sides in system (2.2) equal 0, i.e.,

$$\begin{cases} \mu\rho + \sigma\rho R - \alpha S(E+I) - \mu S = 0, & \text{(3.1a)} \\ \mu(1-\rho) + \sigma(1-\rho)R - \beta L(E+I) - \mu L = 0, & \text{(3.1b)} \\ \alpha S(E+I) + \beta L(E+I) - \delta E - \mu E = 0, & \text{(3.1c)} \\ \delta E - \gamma I - \mu I = 0, & \text{(3.1d)} \\ \gamma I - \sigma R - \mu R = 0. & \text{(3.1e)} \end{cases}$$

The disease-free equilibrium point represents the state in which the system eventually converges to a disease-free state. Therefore, the disease-free equilibrium point $E_0 = (\rho, 1-\rho, 0, 0, 0)$ can be solved immediately by letting $E = 0$, $I = 0$, on the basis of Eq (3.1). In addition, the unique endemic

equilibrium $E_* = (S^*, L^*, E^*, I^*, R^*)$ where

$$\begin{cases} S^* = \dfrac{\mu\rho + \sigma\rho\dfrac{\gamma}{\sigma+\mu}I^*}{\alpha\dfrac{\gamma+\mu}{\delta}I^* + \alpha I^* + \mu}, \\ L^* = \dfrac{\mu(1-\rho) + \sigma(1-\rho)\dfrac{\gamma}{\sigma+\mu}I^*}{\beta\dfrac{\gamma+\mu}{\delta}I^* + \beta I^* + \mu}, \\ E^* = \dfrac{\gamma+\mu}{\delta}I^*, \\ R^* = \dfrac{\gamma}{\sigma+\mu}I^*, \end{cases} \tag{3.2}$$

and

$$I^* = -\frac{\delta}{K}\left(Q\alpha + \beta\mu^3 + \beta(\sigma+\delta+\gamma)\mu^2 + C\beta\mu + \beta\sigma\delta\rho\gamma + \sqrt{U}\right),$$

$$\begin{aligned} A = &(((\alpha-\mu)\beta - \alpha\mu)(\alpha-\beta)\rho - \alpha((\alpha+\mu)\beta - \alpha\mu))\sigma \\ &+ 2(\alpha\beta\rho + (-\alpha/2 - \mu/2)\beta + 1/2\alpha\mu)\mu(\alpha-\beta), \end{aligned}$$

$$B = 4\alpha\beta\mu(\alpha-\beta)\rho + ((\alpha+\mu)\beta - \alpha\mu)^2,$$

$$C = (\gamma+\delta)\sigma + \delta\gamma,$$

$$D = ((\alpha-\beta)\rho - \alpha)^2\sigma^2 - 2((\alpha+\beta)\rho - \alpha)\mu(\alpha-\beta)\sigma + \mu^2(\alpha-\beta)^2,$$

$$K = 2(\gamma+\mu+\delta)\alpha\left(\mu^2 + (\sigma+\delta+\gamma)\mu + C\right)\beta,$$

$$Q = \mu^3 + (-\beta+\sigma+\delta+\gamma)\mu^2 + ((-\sigma-\delta-\gamma)\beta + C)\mu - \sigma((\gamma+\delta)\beta + \delta\gamma(-1+\rho)),$$

$$\begin{aligned} U = &\left(D\gamma^2 + 2(\sigma+\mu)A\gamma + B(\sigma+\mu)^2\right)\delta^2 \\ &+ 2(A\gamma + B(\sigma+\mu))(\gamma+\mu)(\sigma+\mu)\delta + B(\gamma+\mu)^2(\sigma+\mu)^2. \end{aligned}$$

As a key index to measure the disease epidemic, the basic reproduction number can be calculated by the next generation matrix method [32]. Here, the next generation matrix

$$\begin{aligned} P = FV^{-1} &= \begin{pmatrix} \alpha\rho + \beta(1-\rho) & \alpha\rho + \beta(1-\rho) \\ 0 & 0 \end{pmatrix} \begin{pmatrix} \frac{1}{\delta+\mu} & 0 \\ \frac{\delta}{(\delta+\mu)(\gamma+\mu)} & \frac{1}{\gamma+\mu} \end{pmatrix} \\ &= \begin{pmatrix} \frac{\alpha\rho+\beta(1-\rho)}{\delta+\mu} + \frac{\delta(\alpha\rho+\beta(1-\rho))}{(\delta+\mu)(\gamma+\mu)} & \frac{\alpha\rho+\beta(1-\rho)}{\gamma+\mu} \\ 0 & 0 \end{pmatrix}, \end{aligned} \tag{3.3}$$

where $F = \begin{pmatrix} \alpha\rho + \beta(1-\rho) & \alpha\rho + \beta(1-\rho) \\ 0 & 0 \end{pmatrix}$ and $V = \begin{pmatrix} \delta+\mu & 0 \\ -\delta & \gamma+\mu \end{pmatrix}$ are the infection matrix and transfer matrix, respectively.

So, the basic reproduction number of system (2.2) is

$$R_0 = \left(\frac{1}{\delta+\mu} + \frac{\delta}{(\delta+\mu)(\gamma+\mu)}\right)(\alpha\rho + \beta(1-\rho)). \tag{3.4}$$

From (3.4), it is easy to get that R_0 is an increasing function of α, β, and ρ and a decreasing function of δ, γ, and μ. Further, the correlation between R_0 and parameters is listed in Table 2, which is easily explained from the propagation diagram shown in Figure 1. To be specific, a higher infected rate leads to the larger basic regeneration number, and thus accelerates the propagation of disease. A higher recovery rate or outbreak rate will reduce the basic regeneration number and thereby controls the spread of disease. These are consistent with the intuitive perception in reality.

Interestingly, the promotion of detecting the asymptomatic infected, equivalently the increase of parameter δ, may prevent the disease propagation. In fact, it has been used to conduct COVID-19 prevention and control as a policy in China. In addition, counter-intuitively, the loss rate σ of immunity does nothing on the basic regeneration number, that is to say, the loss rate of immunity has no influence on the disease propagation.

Table 2. Correlation of parameters with disease controllability (R_0).

Parameters	Relevance
α	Positive correlation
β	Positive correlation
δ	Negative correlation
γ	Negative correlation
μ	Negative correlation
ρ	Positive correlation at the assumption of $\alpha > \beta$

3.2. Stability analysis of SLEIRS model

Theorem 1. If $R_0 < 1$, system (2.2) is globally asymptotically stable at the disease-free equilibrium point. If $R_0 > 1$, system (2.2) is unstable at the disease-free equilibrium point.

Proof. It is easy to get the Jacobian matrix of system (2.2)

$$J = \begin{pmatrix} -\alpha(E+I)-\mu & 0 & -\alpha S & -\alpha S & \sigma\rho \\ 0 & -\beta(E+I)-\mu & -\beta L & -\beta L & \sigma(1-\rho) \\ \alpha(E+I) & \beta(E+I) & \alpha S+\beta L-\delta-\mu & \alpha S+\beta L & 0 \\ 0 & 0 & \delta & -\gamma-\mu & 0 \\ 0 & 0 & 0 & \gamma & -\sigma-\mu \end{pmatrix},$$

and then the Jacobian matrix at the disease-free equilibrium is

$$J(E_0) = \begin{pmatrix} -\mu & 0 & -\alpha\rho & -\alpha\rho & \sigma\rho \\ 0 & -\mu & -\beta(1-\rho) & -\beta(1-\rho) & \sigma(1-\rho) \\ 0 & 0 & \alpha\rho+\beta(1-\rho)-\delta-\mu & \alpha\rho+\beta(1-\rho) & 0 \\ 0 & 0 & \delta & -\gamma-\mu & 0 \\ 0 & 0 & 0 & \gamma & -\sigma-\mu \end{pmatrix}.$$

Obviously, $\lambda_1 = \lambda_2 = -\mu$ are two eigenvalues of $J(E_0)$, and the other eigenvalues are determined by the eigenequation as below:

$$|\lambda E - J^*| = \begin{vmatrix} \lambda-\alpha\rho-\beta(1-\rho)+\delta+\mu & -\alpha\rho-\beta(1-\rho) & 0 \\ -\delta & \lambda+\gamma+\mu & 0 \\ 0 & -\gamma & \lambda+\sigma+\mu \end{vmatrix} = 0. \tag{3.5}$$

Obviously, $\lambda_3 = -\sigma - \mu$ is an eigenvalue, and the other two are the two roots of the following equation:

$$\begin{aligned}&\lambda^2 + [\gamma + \mu - \alpha\rho - \beta(1-\rho) + \delta + \mu]\lambda \\ &+ (\gamma + \mu)[-\alpha\rho - \beta(1-\rho) + \delta + \mu] - \delta[\alpha\rho + \beta(1-\rho)] = 0.\end{aligned}$$

Consider λ_4, λ_5 as the roots, and by using the condition of $R_0 < 1$, it follows that

$$\begin{aligned}\lambda_4 + \lambda_5 &= -[\gamma + 2\mu - \alpha\rho - \beta(1-\rho) + \delta] \\ &< -(\gamma + 2\mu + \delta) + \frac{(\delta+\mu)(\gamma+\mu)}{\gamma+\mu+\delta} \\ &= \frac{(\delta+\mu)(\gamma+\mu) - (\gamma+\mu+\delta)(\gamma+2\mu+\delta)}{\gamma+\mu+\delta} \\ &< 0,\end{aligned}$$

$$\begin{aligned}\lambda_4 \cdot \lambda_5 &= (\gamma+\mu)[-\alpha\rho - \beta(1-\rho) + \delta + \mu] - \delta[-\alpha\rho - \beta(1-\rho)] \\ &> -(\delta+\mu)(\gamma+\mu) + \delta[\alpha\rho + \beta(1-\rho)] + (\delta+\mu)(\gamma+\mu) - \delta[-\alpha\rho - \beta(1-\rho)] \\ &= 0.\end{aligned}$$

So, both λ_4 and λ_5 are less than 0, and thus all eigenvalues of the Jacobian at the disease-free equilibrium point are negative. According to the Lyapunov stability criterion, system (2.2) is locally asymptotically stable at the disease-free equilibrium point when $R_0 < 1$.

One the other hand, let $\boldsymbol{y} = (E, I)^{\mathrm{T}}$, and it is easy from system (2.2) to get that

$$\frac{d\boldsymbol{y}}{dt} = \begin{pmatrix}\alpha S + \beta L - \delta - \mu & \alpha S + \beta L \\ \delta & -\gamma - \mu\end{pmatrix}\begin{pmatrix}E \\ I\end{pmatrix} \leq \begin{pmatrix}\alpha\rho + \beta(1-\rho) - \delta - \mu & \alpha\rho + \beta(1-p) \\ \delta & -\gamma - \mu\end{pmatrix}\boldsymbol{y} = (F - V)\boldsymbol{y}. \tag{3.6}$$

Select the Lyapunov candidate function

$$M = \boldsymbol{\alpha}^{\mathrm{T}} V^{-1} \boldsymbol{y}, \tag{3.7}$$

where $\boldsymbol{\alpha}$ is the left eigenvector of nonnegative matrix $P = V^{-1}F$ associated with its spectral radius R_0, i.e., $\boldsymbol{\alpha}^{\mathrm{T}} V^{-1} F = R_0 \boldsymbol{\alpha}^{\mathrm{T}}$, and it is a positive vector according to the property of Perron theory. Then, one has

$$\begin{aligned}\frac{dM}{dt} &= \boldsymbol{\alpha}^{\mathrm{T}} V^{-1} \frac{d\boldsymbol{y}}{dt} \leq \boldsymbol{\alpha}^{\mathrm{T}} V^{-1}(F - V)\boldsymbol{y} \\ &= \boldsymbol{\alpha}^{\mathrm{T}} V^{-1} F \boldsymbol{y} - \boldsymbol{\alpha}^{\mathrm{T}} \boldsymbol{y} \\ &\leq (R_0 - 1)\boldsymbol{\alpha}^{\mathrm{T}} \boldsymbol{y}.\end{aligned} \tag{3.8}$$

Thus, $\frac{dM}{dt} \leq 0$ when $R_0 < 1$, and the equality holds if and only if $\boldsymbol{y} = 0\,(E = 0, I = 0)$. According to the LaSalle invariance principle, the state of system (2.2) starting from the point in the positive invariant set Ω will tend to the disease-free equilibrium point, namely, system (2.2) is globally asymptotically stable at the disease-free equilibrium point.

4. Numerical simulations of SLEIRS model

4.1. Simulations for dynamical behaviors

In this section, we will verify the above theoretical results and analyze the influence of parameters on the disease propagation dynamics. Here, initial populations of compartments in system (2.1) are set as $N = 1000$, $I = 100$, $R = 0$, $L = 300$, $S = 500$, and $E = 100$, which is easily rewritten into the normalized form for system (2.2). For the asymptotically stable case of $R_0 < 1$, we take two sets of parameters: (a) $\alpha = 0.2$, $\beta = 0.1$, (b) $\alpha = 0.08$, $\beta = 0.06$, and $\gamma = 0.8$, $\delta = 0.15$, $\rho = 0.3$, $\mu = 0.005$, $\sigma = 0.1$. Then, $R_0 = 0.995$, and $R_0 = 0.505$, respectively, according to the equality (3.4). The evolution curves for each compartment are obtained based on the aforementioned parameters, following the numerical solution of system (2.2) using the ODE method. As shown in Figure 2, the infected state $I(t)$, as well as the asymptomatic infected state $E(t)$, gradually converges to zero as time goes on, and the state of system (2.1) tends to the disease-free equilibrium point. Furthermore, a comparison of (a) and (b) demonstrates that both $I(t)$ and $E(t)$ exhibit a faster convergence to 0 in the plot of (b) than in (a), corresponding to the smaller R_0, thereby corroborating the theoretical results.

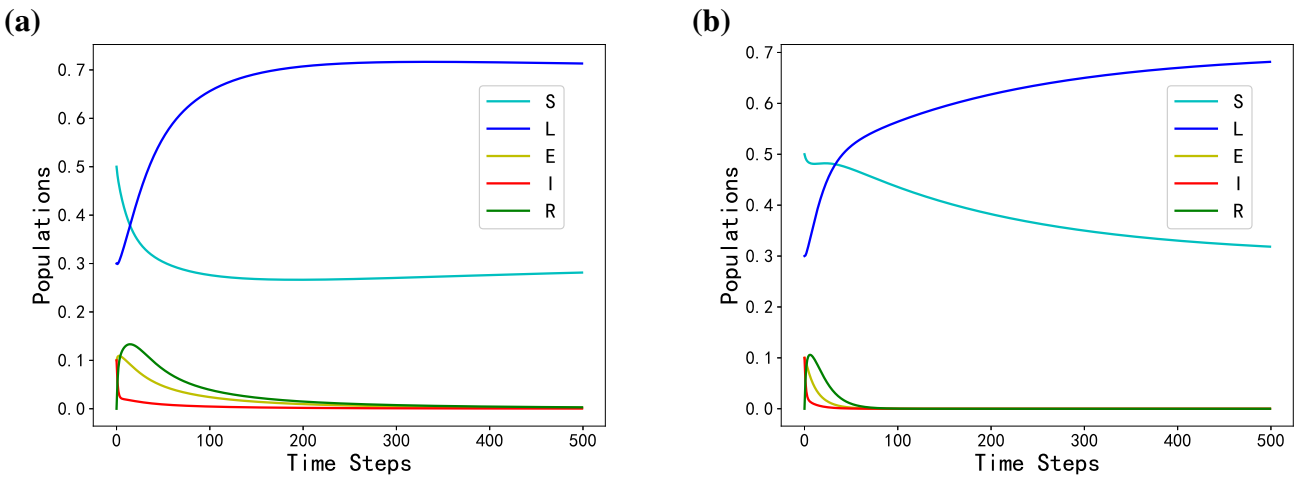

Figure 2. Evolution curves of all states in system (2.2) with $R_0 < 1$. Two sets of parameters: (a) $\alpha = 0.2$, $\beta = 0.1$, (b) $\alpha = 0.08$, $\beta = 0.06$, and $\gamma = 0.8$, $\delta = 0.15$, $\rho = 0.3$, $\mu = 0.005$, $\sigma = 0.1$. Then, $R_0 = 0.995$, and $R_0 = 0.505$, respectively.

On the other hand, for the unstable case of $R_0 > 1$, we also take two sets of parameters: (a) $\alpha = 0.2$, $\beta = 0.1$, (b) $\alpha = 0.5$, $\beta = 0.4$, and $\gamma = 0.3$, $\delta = 0.15$, $\rho = 0.3$, $\mu = 0.005$, $\sigma = 0.1$. Then, $R_0 = 1.251$, and $R_0 = 4.139$, respectively. From simulation results shown in Figure 3, it is clear that the state finally tends to the endemic equilibrium point determined by (3.6), and the larger R_0 is represented by the (b) plot, where both $I(t)$ and $E(t)$ stabilize to higher values and converge more rapidly than in (a). This demonstrates that the larger R_0 speeds up the disease propagation and causes the system to ultimately converge to a larger endemic equilibrium point.

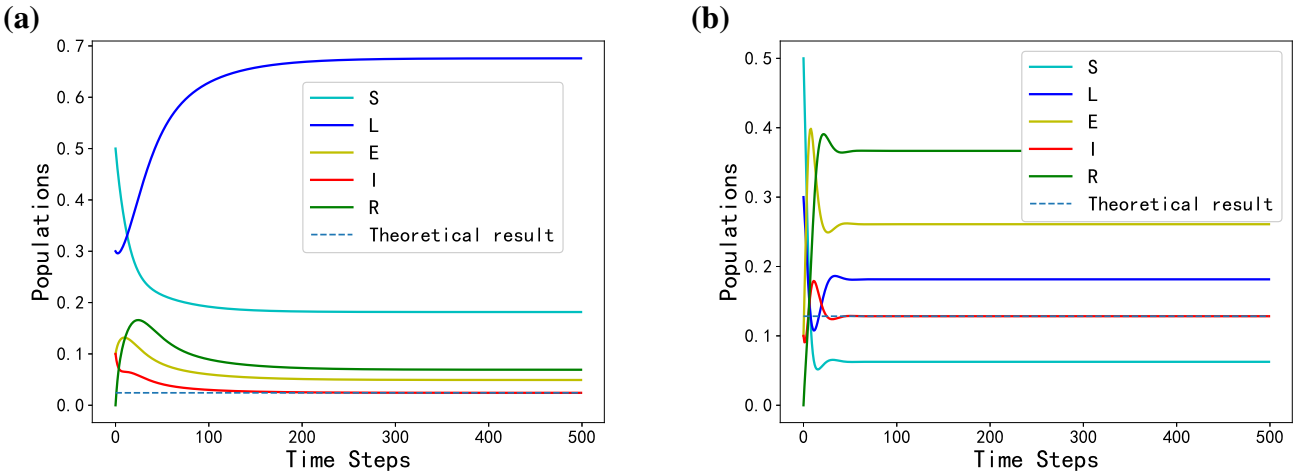

Figure 3. Evolution curves of all states in system (2.2) with $R_0 > 1$. Two sets of parameters: (a) $\alpha = 0.2, \beta = 0.1$, (b) $\alpha = 0.5, \beta = 0.4$, and $\gamma = 0.3, \delta = 0.15, \rho = 0.3, \mu = 0.005, \sigma = 0.1$. Then, $R_0 = 1.251$, and $R_0 = 4.139$, respectively.

Next, for analyzing the influence of parameters on the disease transmission, we take the underlying setting of parameters: $\alpha = 0.2, \beta = 0.1, \gamma = 0.8, \delta = 0.1, \rho = 0.3, \mu = 0.005$, and $\sigma = 0.1$. On that basis let one parameter therein vary in the interval $[0, 1]$ while fixing other parameters. A numerical simulation is conducted using ODE, with the resulting images plotted by taking the number of E, I after stabilization of each set of parameters as vertical coordinates and the controlled variables as horizontal coordinates. Simulation results shown Figure 4 are well consistent with those in Table 2, where the equilibrium state of $E + I$ increases with the increase of α, β, and ρ (see Figure 4(a,b,f)), respectively, and the equilibrium state decreases with the increase of δ, γ, and μ (see Figure 4(c,d,e), respectively. By the way, for the cases of α, β, δ, and μ, it takes $R_0 = 1$ at $\alpha = 0.078, \beta = 0.048, \delta = 0.149$, and $\mu = 0.045$ (marked in the big dot in the curves), respectively, and it does not take $R_0 = 1$ at the interval of $[0, 1]$ for the cases of γ and ρ.

From Figure 4 (c,d,e), it is evident that the equilibrium state of $E + I$ decreases quickly as the outbreak rate δ and the recovered rate γ rise, respectively, whereas the infected amount increases slightly at the beginning and then decreases as the outbreak rate δ rises. This implies that a small outbreak rate can facilitate the disease transmission, and more asymptomatic individuals are transferred into the infected and subsequently into the recovered when the outbreak rate is larger than an appropriate value, thereby preventing the disease propagation. Based on the theoretical and numerical analysis, it shows that detecting the asymptomatic infected is a good measure to prevent and control the disease transmission.

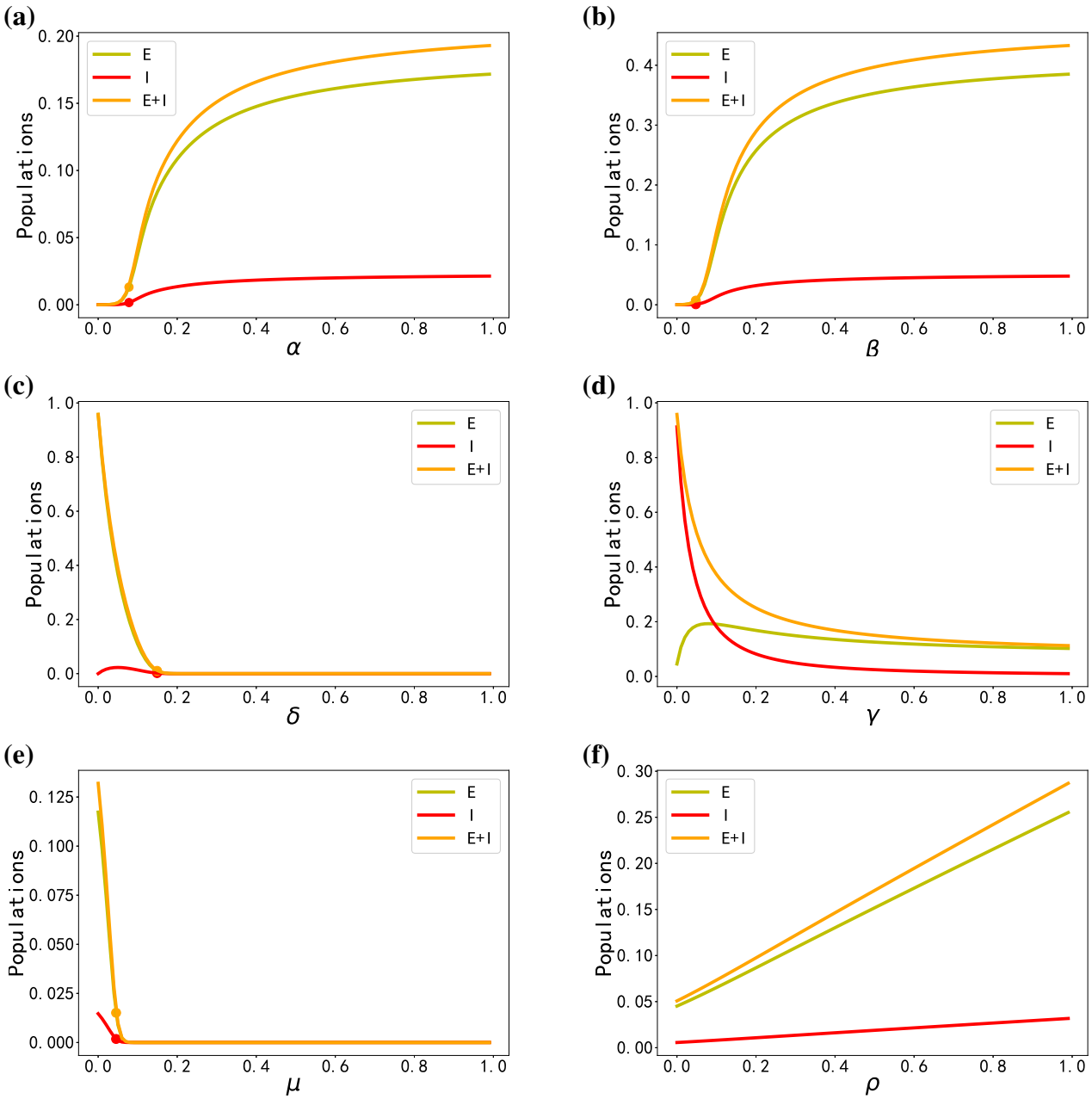

Figure 4. Effects of the parameters (a) α, (b) β, (c) δ, (d) γ, (e) μ and (f) ρ on the number of infected individuals (I) and the number of asymptomatic infections (E).

4.2. Prediction and parameter estimation of model based on the real epidemic data

In this section, we use the real epidemic data released by the National Health Commission from 2021 to 2022, as well as the vaccination data provided by Our World in Data [33], to estimate the parameters in the SLEIRS model, and we make the prediction based on the model with estimated parameters.

To begin with, we normalize the data for better model training and optimization at the same scale and determine two uncertain compartments (the low-risk amount and the asymptomatic infected

amount), as well as the easily-estimated parameters (the birth-death rate and the loss rate of immunity). Here, the number of vaccinated individuals is taken as the low-risk population, since COVID-19 epidemic investigations show that the vaccinated population may be infected with lower rate in general. According to the relevant information that the individual has about a half-one-year immunization period after being cured, the newly-increased asymptomatic infected amount accumulated for the last 180 days is taken as the existing asymptomatic infected amount. On the other hand, the birth-death rate μ is set at between 6.77‰ and 7.52‰ according to the 6.77‰ death rate and the 7.52‰ birth rate in 2021 and 2022 released by the National Bureau of Statistics of China. Furthermore, the "Our World in Data" report [33] indicates that the immunization rate is approximately 0.6. Consequently, the distribution of susceptible and low-risk individuals within the population is constrained to the range [0.5, 0.69].

System (2.2) comprises 7 parameters. In order to identify the parameters in the model using real epidemic data, we employ a process of minimizing the error between the real data and the numerical solution of the model with the given parameters. This is essentially an optimization problem. The error function is defined as follows:

$$\arg\min_{P} \sum_{i=1}^{N} \frac{\left\| f_i(t) - f_i^s(t,P) \right\|}{\|f_i(t)\|},$$

where $f_i(t)$ is the real epidemic data, $f_i^s(t,P)$ is the numerical solution of the ith variable when the parameter set is P, N is the number of variables, and $\|\cdot\|$ is the norm (here a vector 2-norm) The numerical solution of the ODEs is solved by ode15s. The optimization problem is solved using the particle swarm optimisation (PSO) algorithm.

The PSO algorithm comprises a population of particles, each of which possesses two attributes: Velocity and displacement. During the search process, each particle navigates in the direction of its own judgement, and at the conclusion of the search, it records the optimal position.

Assume a total of M particles, each representing a solution.

The velocity update formula is as follows:

$$v_{id}^{k+1} = \omega v_{id}^{k} + c_1 r_1 \left(p_{id,pbest}^{k} - x_{id}^{k} \right) + c_2 r_2 \left(p_{d,gbest}^{k} - x_{id}^{k} \right).$$

The position update formula is as follows:

$$x_{id}^{k+1} = x_{id}^{k} + v_{id}^{k+1},$$

where v_{id}^{k+1} denotes the velocity vector of particle i in the d-dimension in the kth iteration; x_{id}^{k} denotes the position vector of particle i in the d-dimension in the kth iteration; ω denotes inertia weight; c_1 denotes individual learning factor; c_2 denotes the population learning factor; r_1 and r_2 are random numbers. The variable $p_{id,pbest}^{k}$ represents the historically optimal position of particle i in the dth dimension in the kth iteration, while $p_{d,pbest}^{k}$ denotes the historical optimal position of the population in the kth iteration.

In light of the preceding discussion of the parameters, the initial values of the parameters are set as follows: μ is a random number within the interval $[0.068, 0.0075]$, ρ is a random number within the interval $[0.5, 0.69]$, and the remaining parameters are taken to be random numbers within the interval $[0, 1]$. The parameter boundary conditions are identical to those previously described for the generation of the initial random numbers. The algorithm is implemented in Matlab.

Next, we divide the data into two segments in consideration of the singular property. We use the PSO algorithm to estimate the parameters in the SLEIRS model based on each segment data and then apply the model with estimated parameters to predict the epidemic. Here the first-two-months data is used to train, and the last half-one-month data is used to make the prediction. The parametric results are presented in Table 3.

4.2.1. Estimation and prediction based on the first segment data

The first-two-months data (from December 15, 2021, to February 15, 2022) in the first segment data (from December 15, 2021, to March 1, 2022) is used as the training set, and the PSO algorithm is applied to estimate the parameters in the model. The fitting curves are shown in Figure 5, and the estimated parameters are shown in Table 3, where the estimated $\mu = 0.0075$ is basically consistent with the birth rate in 2021, and the estimated parameters, $\alpha > \beta$, meet the assumption in the SLEIRS model.

With the estimated parameters, the SELIRS model (2.2) is used to predict the state of each compartment in the subsequent half one month (from February 15 to March 1, 2022). As shown in Figure 5, the prediction curves are well consistent with the real data in the first week, and the mean square error of prediction in all states in the half-one-month data is 0.0275%. More importantly, the basic regeneration number in the model with estimated parameters, $R_0 = 1.104282$, implies the mild spread of epidemic, which is basically consistent with the epidemic at that time in China.

Table 3. Lists of estimated parameters in the model.

Parameters	Estimated values (the 1st segment)	Estimated values (the 2nd segment)
α	0.16982	0.10362
β	0.15000	0.07625
γ	0.16552	0.13381
δ	0.99998	0.23227
σ	0.08684	1.446e-09
ρ	0.71169	0.69000
μ	0.00750	0.00680

4.2.2. Estimation and prediction based on the second segment data

Similarly, the first-two-months data (from May 15 to July 15, 2022) in the second segment data (from May 15 to August 1, 2022) is used to fit the model via the PSO algorithm, and the fitting result is shown in Figure 6. Also, the estimated parameters are shown in Table 3, where the estimated $\mu = 0.0068$ is basically consistent with the birth rate in 2022, and the estimated parameters, $\alpha > \beta$, meet the assumption in the SLEIRS model.

Compared with the estimated value of ρ in the first segment data, the estimated value in the second segment data is smaller, implying the population that the recovered transfers to the susceptible becomes less, perhaps due to the fact that more people take the vaccine booster. Also, the estimated values of other parameters in the second segment data are less than those in the first segment data. In particular, the estimated values of both the outbreak rate (δ) and the loss rate of immunity (σ) have sharp declines, showing that the epidemic goes into a good situation.

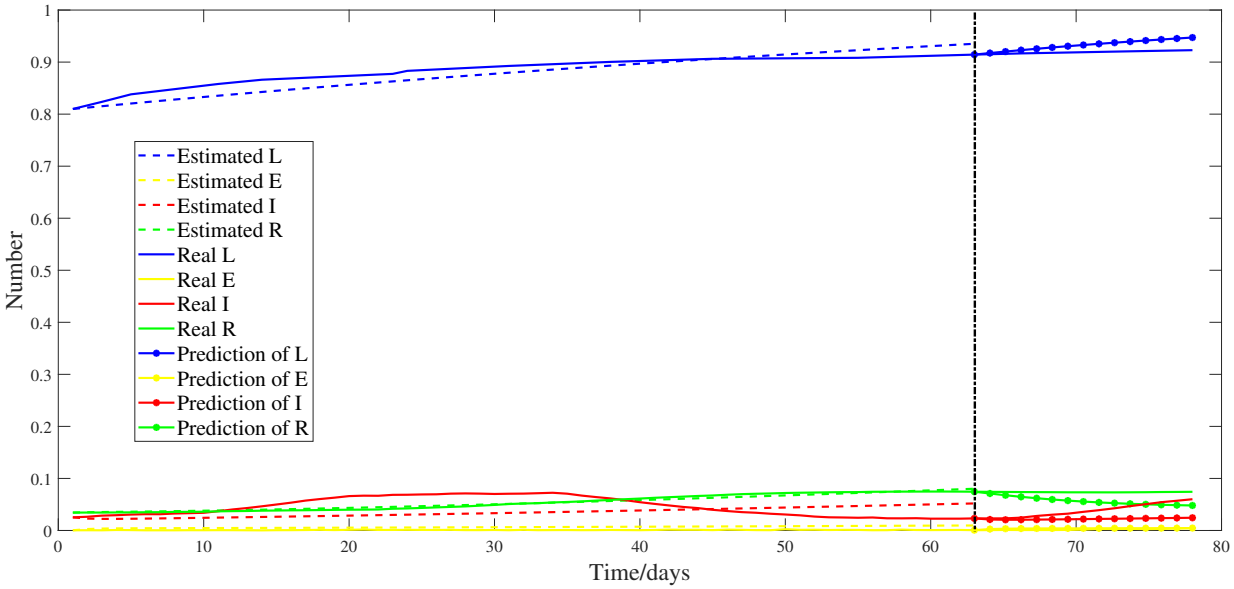

Figure 5. Forecast curve for December 2021 to March 2022 in China.

With the estimated parameters, the SELIRS model (2.2) is used to predict the state of each compartment in the subsequent half one month (from July 15 to August 1, 2022). As shown in Figure 6, the prediction curves are well consistent with the real data in the first week, and the mean square error of prediction in all states in the half-one-month datais 0.0581%. Meanwhile, the basic regeneration number in the model with estimated parameters, $R_0 = 1.055275$, is less than that in the first segment data, implying the epidemic spread is slower than that in the first segment data, which is basically consistent with the fact that the epidemic in 2022 is better than that in 2021.

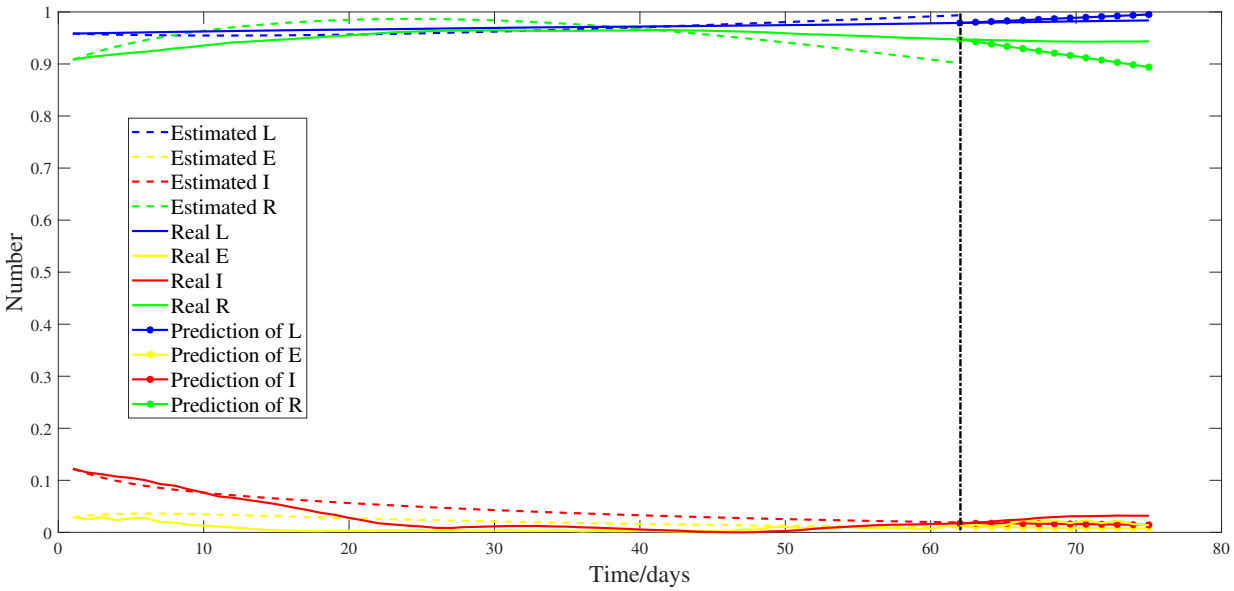

Figure 6. Forecast curve for May to August 2022 in China.

5. Conclusions

In summary, we have developed a new SLEIRS model with the birth-death mechanism for COVID-19 in the post-pandemic era, and we have derived the stability conditions for the disease-free equilibrium, as well as the basic regeneration number. Numerical simulations have validated the theoretical results and have shown that the higher outbreak rate δ is more conducive to prevent the disease propagation, indicating that enhanced detection of the asymptomatic infected is an effective measure to prevent and control the epidemic.

Compared with the SEIR model, the SLIERS model is more suitable for characterizing the state feature of COVID-19 propagation, where the recovered are not permanently immune to COVID-19. Further, some rational cases, such as the birth-death rate, low-risk individuals with self-protection awareness, and the loss of immunity, are integrated into the model.

In a more practical sense, the proposed model has been applied to the real COVID-19 data from 2021 to 2022 in China, and investigations on the parameter estimation and prediction have shown that the results are basically consistent with the epidemic situation at that time in China, to some extent implying the SLEIRS model has good capability in describing the propagation of COVID-19 in the post-pandemic era. Our theoretical and numerical analysis of the proposed may strengthen understanding of the dynamical behavior of epidemic propagation in the post-pandemic era, and provide theoretical support in policy-making for preventing and controlling the epidemic.

Furthermore, the advantages and disadvantages of various algorithms for predicting COVID-19 can be further explored from a data-driven perspective. It would be beneficial to include control variables in the model in order to determine the most effective strategy for eliminating the infection, which will be considered in future work.

Author contributions

Xiaoying Pan: Investigation, Visualization, Software, Writing-Original Draft, Validation, Writing-Reviewing and Editing; Longkun Tang: Conceptualization, Methodology, Supervision and Writing. All authors have read and approved the final version of the manuscript for publication.

Use of AI tools declaration

The authors declare they have not used Artificial Intelligence (AI) tools in the creation of this article.

Acknowledgments

This work was supported in part by the National Natural Science Foundation of China under Grants 62076104, 61573004, 11901215 and in part by the Natural Science Foundation of Fujian Province under Grants 2019J01065 and 2021J01303.

Conflict of interest

The authors declare no conflict of interest.

References

1. E. F. Arruda, D. H. Pastore, C. M. Dias, S. S. Das, Modelling and optimal control of multi strain epidemics, with application to COVID-19, *Plos One*, **16** (2021), e0257512. https://doi.org/10.1371/journal.pone.0257512
2. Q. Liu, D. Jiang, T. Hayat, B. Ahmad, Analysis of a delayed vaccinated sir epidemic model with temporary immunity and lévy jumps, *Nonlinear Anal. Hybrid Syst.*, **27** (2018), 29–43. https://doi.org/10.1016/j.nahs.2017.08.002
3. W. Li, X. Xue, L. Pan, T. Lin, W. Wang, Competing spreading dynamics in simplicial complex, *Appl. Math. Comput.*, **412** (2022), 126595. https://doi.org/10.1016/j.amc.2021.126595
4. C. Xia, Z. Wang, C. Zheng, Q. Guo, Y. Shi, M. Dehmer, et al., A new coupled disease-awareness spreading model with mass media on multiplex networks, *Inf. Sci.*, **471** (2019), 185–200. https://doi.org/10.1016/j.ins.2018.08.050
5. L. Tang, Y. Zhou, L. Wang, S. Purkayastha, L. Zhang, J. He, et al., A review of Multi-Compartment infectious disease models, *Int. Stat. Rev.*, **88** (2020), 462–513. https://doi.org/10.1111/insr.12402
6. H. Joshi, M. Yavuz, Transition dynamics between a novel coinfection model of fractional-order for COVID-19 and tuberculosis via a treatment mechanism, *European Phys. J. Plus*, **138** (2023), 468. https://doi.org/10.1140/epjp/s13360-023-04095-x
7. M. A. Achterberg, B. Prasse, L. Ma, S. Trajanovski, M. Kitsak, P. Van Mieghem, Comparing the accuracy of several network-based COVID-19 prediction algorithms, *Int. J. Forecast.*, **38** (2020), 489–504. https://doi.org/10.1016/j.ijforecast.2020.10.001
8. F. Petropoulos, S. Makridakis, N. Stylianou, COVID-19: Forecasting confirmed cases and deaths with a simple time series model, *Int. J. Forecast.*, **38** (2022), 439–452. https://doi.org/10.1016/j.ijforecast.2020.11.010
9. S. Lalmuanawma, J. Hussain, L. Chhakchhuak, Applications of machine learning and artificial intelligence for Covid-19 (SARS-CoV-2) pandemic: A review, *Chaos Solit. Fract.*, **139** (2020), 110059. https://doi.org/10.1016/j.chaos.2020.110059
10. P. Wang, X. Zheng, J. Li, B. Zhu, Prediction of epidemic trends in COVID-19 with logistic model and machine learning technics, *Chaos Solit. Fract.*, **139** (2020), 110058. https://doi.org/10.1016/j.chaos.2020.110058
11. S. Rezapour, S. Etemad, R. P. Agarwal, K. Nonlaopon, On a Lyapunov-Type inequality for control of a si-Model thermostat and the existence of its solutions, *Mathematics*, **10** (2022), 4023. https://doi.org/10.3390/math10214023
12. K. Shah, A. Ali, S. Zeb, A. Khan, M. A. Alqudah, T. Abdeljawad, Study of fractional order dynamics of nonlinear mathematical model, *Alex. Eng. J.*, **61** (2022), 11211–11224. https://doi.org/10.1016/j.aej.2022.04.039

13. A. Turab, W. Sintunavarat, A unique solution of the iterative boundary value problem for a second-order differential equation approached by fixed point results, *Alex. Eng. J.*, **60** (2021), 5797–5802. https://doi.org/10.1016/j.aej.2021.04.031

14. H. Hethcote, Z. E. Ma, S. B. Liao, Effects of quarantine in six endemic models for infectious diseases, *Math. Biosci.*, **180** (2002), 141–160. https://doi.org/10.1016/S0025-5564(02)00111-6

15. W. O. Kermack, A. G. Mckendrick, A contribution to the mathematical theory of epidemics, *Proc. Royal Society A*, **115** (1927), 700–721. https://doi.org/10.1098/rspa.1927.0118

16. S. Kim, Y. J. Kim, K. R. Peck, E. Jung, School opening delay effect on transmission dynamics of coronavirus disease 2019 in Korea: Based on mathematical modeling and simulation study, *J. Korean medical sci.*, **35** (2020), e143. https://doi.org/10.3346/jkms.2020.35.e143

17. T. Fayeldi, R. Dinnullah, Covid-19 sir model with nonlinear incidence rate, *J. Phys. Conf. Series*, **1869** (2021), 012113. https://doi.org/10.1088/1742-6596/1869/1/012113

18. D. Efimov, R. Ushirobira, On an interval prediction of COVID-19 development based on a SEIR epidemic model, *Annual Rev. Contr.*, **51** (2021), 477–487. https://doi.org/10.1016/j.arcontrol.2021.01.006

19. M. K. Arti, Mathematical modeling of covid-19 and prediction of upcoming wave, *IEEE J. Selected Top. Signal Proc.*, **16** (2022), 300–306. https://doi.org/10.1109/JSTSP.2022.3152674

20. I. Cooper, A. Mondal, C. G. Antonopoulos, A SIR model assumption for the spread of COVID-19 in different communities, *Chaos Solit. Fract.*, **139** (2020), 110057. https://doi.org/10.1016/j.chaos.2020.110057

21. N. Piovella, Analytical solution of seir model describing the free spread of the covid-19 pandemic, *Chaos Solit. Fract.*, **140** (2020), 110243. https://doi.org/10.1016/j.chaos.2020.110243

22. B. Ivorra, M. Ferrandez, M. Vela-Pérez, A. Ramos, Mathematical modeling of the spread of the coronavirus disease 2019 (COVID-19) taking into account the undetected infections. The case of China, *Commun. Nonlinear Sci. Numer. Simu.*, **88** (2020), 105303. https://doi.org/10.1016/j.cnsns.2020.105303

23. F. Yin, J. Lü, X. J. Zhang, X. Xia, J. H. Wu, COVID-19 information propagation dynamics in the Chinese Sina-microblog, *Math. Biosci. Eng.*, **17** (2020), 2676–2692. https://doi.org/10.3934/mbe.2020146

24. W. Sintunavarat, A. Turab, Mathematical analysis of an extended SEIR model of COVID-19 using the ABC-fractional operator, *Math. Comput. Simul.*, **198** (2022), 65–84. https://doi.org/10.1016/j.matcom.2022.02.009

25. A. F. Rihan, M. Q. Al-Mdallal, J. H. AlSakaji, A. Hashish, A fractional-order epidemic model with time-delay and nonlinear incidence rate, *Chaos Solit. Fract.*, **126** (2019), 97–105. https://doi.org/10.1016/j.chaos.2019.05.039

26. L. Padilla, R. Fygenson, S. C. Castro, E. Bertini, Multiple forecast visualizations (MFVs): Trade-offs in trust and performance in multiple COVID-19 forecast visualizations, *IEEE T. Visualiz. Comput. Graph.*, **29** (2023), 12–22. https://doi.org/10.1109/TVCG.2022.3209457

27. S. He, Y. Peng, K. Sun, SEIR modeling of the COVID-19 and its dynamics, *Nonlinear Dyn.*, **101** (2020), 1667–1680. https://doi.org/10.1007/s11071-020-05743-y

28. S. Annas, M. I. Pratama, M. Rifandi, W. Sanusi, S. Side, Stability analysis and numerical simulation of SEIR model for pandemic COVID-19 spread in Indonesia, *Chaos Solit. Fract.*, **139** (2020), 110072. https://doi.org/10.1016/j.chaos.2020.110072

29. S. Zhao, H. Chen, Modeling the epidemic dynamics and control of covid-19 outbreak in china, *Quant. Bio.*, **8** (2020), 11–19. https://doi.org/10.1007/s40484-020-0199-0

30. W. Raslan, Fractional mathematical modeling for epidemic prediction of covid-19 in egypt, *Ain Shams Eng. J.*, **12** (2021), 3057–3062. https://doi.org/10.1016/j.asej.2020.10.027

31. F. A. Rihan, H. J. Alsakaji, Dynamics of a stochastic delay differential model for COVID-19 infection with asymptomatic infected and interacting peoples: Case study in the UAE, *Resul. Phys.*, **28** (2021), 104658. https://doi.org/10.1016/j.rinp.2021.104658

32. P. V. D. Driessche, J. Watmough, Reproduction numbers and sub-threshold endemic equilibria for compartmental models of disease transmission, *Math. Biosci.*, **180** (2002), 29–48. https://doi.org/10.1016/S0025-5564(02)00108-6

33. **Online content:** *The Global Change Data Lab*, Our World in Data, 2024. Available from: `https://ourworldindata.org/`

AIMS Press